NASA Technical Memorandum 87095

NASA-TM-87095 19860006762

Study of Ice Accretion on Icing Wind Tunnel Components

James E. Newton and William Olsen
Lewis Research Center
Cleveland, Ohio

Prepared for the
Twenty-fourth Aerospace Sciences Meeting
sponsored by the American Institute of Aeronautics and Astronautics
Reno, Nevada, January 6–8, 1986

NASA

STUDY OF ICE ACCRETION ON ICING WIND TUNNEL COMPONENTS

James E. Newton and William Olsen
National Aeronautics and Space Administration
Lewis Research Center
Cleveland, Ohio 44135

SUMMARY

In a closed loop icing wind tunnel the icing cloud is simulated by introducing tiny water droplets through an array of nozzles upstream of the test section. This cloud will form ice on all tunnel components (e.g., turning vanes, inlet guide vanes, fan blades, and the heat exchanger) as the cloud flows around the tunnel. These components must have the capacity to handle their icing loads without causing significant tunnel performance degradation during the course of an evening's run. To aid in the design of these components for the proposed Altitude Wind Tunnel (AWT) at NASA Lewis Research Center the existing Icing Research Tunnel (IRT) was used to measure icing characteristics of the IRT's components. The results from the IRT were scaled to the AWT to account for the AWT's larger components and higher velocities. The results showed that from 90 to 45 percent of the total spray cloud froze out on the heat exchanger. Furthermore, the first set of turning vanes downstream of the test section, the FOD screen and the fan blades showed significant ice formation. The scaling showed that the same results would occur in the AWT.

INTRODUCTION

The AWT proposed by NASA Lewis will be designed to perform aircraft icing tests. In the normal operation of such closed loop icing wind tunnels, ice accretion occurs on various tunnel components causing losses in tunnel performance capability, e.g., excessive total pressure losses. Occasionally such losses will require tunnel shutdown. To avoid tunnel shutdown in the AWT it is essential that the tunnel components be designed so they can handle their expected icing loads without losing a significant portion of the tunnel performance. To meet the above requirements for the design of AWT components an ice accretion study was performed on tunnel components in the existing IRT at NASA Lewis. The AWT will be similar in design to the IRT, however the AWT will be larger and have higher Mach numbers.

In a closed loop icing wind tunnel like the IRT and the proposed AWT liquid water, in the form of tiny droplets, is introduced into the chilled airstream through an array of air atomizing nozzles at the bellmouth to the test section. See figures 1 and 2 for the schematic layouts of the IRT and the AWT. Once introduced into the tunnel the droplets quickly reach the surrounding air temperature and will form ice on any object on which they impinge. The tunnel components which will accrete ice, starting downstream of the test section, are the first and second sets of turning vanes (vanes A and B in IRT), the foreign object damage (FOD) screen, the inlet guide vanes (IGVs), the fan blades, the third set of turning vanes, and the heat exchanger. In addition frost due to water vapor can form on any cold surface in the tunnel.

The freeze out (water and vapor) on the heat exchanger increases its pressure drop and decreases its overall heat transfer coefficient. Thus to compensate for the aerodegradation and reduced cooling efficiency the fan power must be increased and refrigerant temperature must be reduced. Ultimatelly the freeze out will cause a termination of the run because velocity and temperature can no longer be held. In addition the ice build up on the turning vanes, screens, and fan blades will add to the overall tunnel pressure drop and component drag loads, thus creating poor flow quality.

A component ice accretion study was necessary since no prior data existed on the contribution of each tunnel component in removing the spray cloud nor on characteristic ice shapes on the various tunnel components. Furthermore, there were no collection efficiency curves for the turning vanes. All three pieces of information are necessary in order to provide a basis from which tunnel component ice protection systems can be designed. The IRT components incorporated into the study included the turning vanes, IGVs, fan blades, and the heat exchanger.

The test covered a wide range of drop sizes while keeping the total temperature and indicated test section velocity at -12 °C (+10 °F) and 67 m/sec (150 mph) respectively. Four drop sizes were run, varying the drop volume median drop sizes from less than 10 to 45 μm.

The data presented below includes characteristic ice shapes on the tunnel components, the overall total collection efficiency curve for the first set of turning vanes downstream of the test section, and the overall mass distribution of ice among the tunnel components. In addition the mass distribution was projected to the AWT to account for its larger size and higher velocities.

NOMENCLATURE

C	cord length, m
$C_{D,CLEAN}$	turning vane loss coefficient clean
$C_{D,ICE}$	turning vane loss coefficient iced
DVM	droplet volume medium, μm
d	drop size, μm
E	total overall collection efficiency
Ko	dimensionless inertia parameter
LWC	liquid water content, g/m^3
M	test section Mach number
MC	total mass of cloud, kg
MF	mass of ice on fan blades, kg

MT	blade tip Mach number
MV	mass of ice on turning vanes, kg
NB	number of fan blades
T	static temperature, c
To	total temperature, c
V	test section velocity, m/s
W	mass accumulation rate, kg/s
τ	accretion time, min

PROCEDURE AND APPARATUS

The IRT is a closed loop refrigerated atmospheric total pressure wind tunnel. Figure 1 shows the schematic of the IRT. The IRT has a 1.8 m (6 ft) high by 2.7 m (9 ft) wide test section, and a maximum empty test section velocity of 134 m/sec (300 mph). The refrigerator has a capacity to cool the air down to a total temperature of -29 °C (-20 °F). Natural cloud conditions are simulated by an array of 77 air atomizing nozzles located upstream of the contraction to the test section. These nozzles can produce a range of drop volume median (DVM) drop sizes from less than 10 to 45 μm. The liquid water content (LWC) can vary from 0.3 to 3.0 g/m^3. Not all combinations of DVM and LWC are possible.

The IRI components incorporated into the ice accretion study were turning vanes A and B, the FOD screen, IGVs, the fan blades, turning vanes C, and the heat exchanger. The locations of each of these components are identical to those in the AWT, except for the heat exchanger. As will be shown later, this difference proves irrelevent. Figure 2 illustrates the component positions in the AWT.

After a specific icing time, ice accretion measurements were made in two different ways on the tunnel components. Ice shapes on turning vanes A and B were obtained by making cross-sectional cuts in the ice on the 12th turning vane from the inside corner and 2 ft down from the center. From these cuts a tracing of the ice shapes were made on cardboard templates. The amount of mass accreted on these two sets of turning vanes was found by passing steam through the vanes, collecting the water and ice falling from the vanes, and then weighing the resulting mass of ice and water. All drains and holes were covered to prevent drainage of water. The mass of ice accreted on the FOD screen was included with the mass of ice on turning vanes B. Lacking a means of removing ice from on the IGVs and fan blades, a different method was invoked for finding the mass of ice. The procedure involved making cross-sectional cuts in the ice, tracing the ice shape, and by using both the density of ice, 890 kg/m^3, and relative uniformity of the ice accretion the mass was determined. Note that for the IGVs only one cut was necessary since the ice was relatively uniform. However, the fan blades required three cuts due to the radial variation of the ice thickness. Turning vanes C accreted no ice for the four cases run, thus requiring no ice accretion measurements. Finally the amount of cloud

removed by the heat exchanger was assumed to be the remaining portion of the cloud. This assumption proved reasonable since no ice was observed on either turning vanes D nor the fine mesh turbulence screen located at the spray bars.[1]

TEST CONDITIONS

The test covered four different spray conditions. For each spray condition the test section indicated velocity and total temperature were kept at 67.1 m/sec (150 mph) and -12 °C (+10 °F). The DVM sprays run were 45, 30, 15 and an estimated size of less than 10 μm.[2] For the 45, 30 and 15 μm DVM sprays the total cloud water content, (LWC) x (V) x (τ), was held constant. By error, (LWC) x (V) x (τ) was not the same for the less than 10 μm DVM spray. Table I lists the conditions run.

RESULTS AND DISCUSSION

Pictorial Walk Around IRT

Before delving into the heart of the test results, a pictorial walk around the IRT is first helpful as shown in figures 3 to 11. These photographs will give a qualitative understanding for those components requiring some form of ice protection, the relative role each component plays in removing the icing cloud, and the effectiveness of deicing turning vanes by merely passing steam through the vanes.

The photographs are from a 40 min icing spray with an indicated test section velocity of 67.1 m/sec (150 mph), a liquid water content of 1.36 g/m^3, and a total temperature of -12 °C (10 °F). The ice shapes are from 30 and 15 μm DVM sprays. The pictorial walk will begin at turning vanes A and end at the heat exchanger. Figure 3 shows the ice accreted on turning vanes A at the leading edge and pressure surface on the 12th turning vane from the inside corner. The ice was glaze at both the leading edge and pressure surface. A thin layer of frost formed on the suction surface. Figure 4 demonstrates that the ice accretion on turning vanes A was not uniform. Although this figure was taken from a different icing condition it, nevertheless, accurately represents the distribution found in all the cases run. The ineffectiveness of passing steam through turning vanes as a form of deicing is shown in figure 5. The photograph strongly suggests that this form of deicing turning vanes was inadequate. The ice melted from the top, down and took roughly 30 min to entirely deice.

---

[1]The fine mesh screen was 316 stainless steel double crimped square mesh with 12-mesh/linear inch and 0.023 in. gauge wire. The screen was 0.9 m by 0.9 m (4 by 4 ft.) in size.

[2]The less than 10 μm spray fell below existing calibration curves. The instrument used for calibration did not have the capability of accurately measuring the small droplets present in the less than 10 μm sprays.

Ice accretion on turning vanes B and the FOD screen are shown in figures 6 and 7. Figure 6 shows the leading edge and pressure surface ice on the 12th turning vane from the inside corner. The ice was rime on both the leading edge and pressure surface. The most likely explanation for the formation of rime ice on vanes B when glaze ice formed on vanes A is that vanes A removed a high percentage of large drops. Thus, the smaller drops, i.e., lower DVM cloud, reaching vanes B would produce rime ice (ref. 1). Like turning vanes A, turning vanes B also formed frost on the suction surface and deiced in the same manner. The ice on the FOD screen is shown in figure 7.

Moving on to the IGVs and fan blades, one can see that the amount of ice accreted was reduced substantially from the first two sets of turning vanes. Figure 8 shows that very little ice accreted on the IGVs the ice was rime and about 3 mm thick. Figure 9 shows the ice accretion on the fan blades near the fan hub. The ice was a mixture of glaze and rime ice (glaze in the stagnation region) and is 22 mm thick at the stagnation point.

Turning vanes C did not accrete any ice as shown in figure 10. However, not all of the cloud was removed at this point. Figure 11 shows the ice formed on the heat exchanger fins and coils. The ice accretion was uniform over the entire heat exchanger area.

For all the cases run no ice formed on either turning vanes D nor the fine mesh turbulence screen. This evidence implied that the heat exchanger removed the remaining portion of the cloud.

Three observations follow from the pictorial walk around the IRT. First, some form of ice protection is needed for the first and perhaps second sets of turning vanes, and the fan blades for the AWT. Second, deicing turning vanes by merely passing steam through them is inadequate. Third, the photographs indicate that a large portion of the cloud was removed by the time it reached turning vanes C. This last observation was strictly qualitative and needed to be substantiated. Thus, the overall mass distribution of ice among the tunnel components was found in the IRT. As the reader will see from the results reported below, the third observation was not a reality at all, but rather an illusion.

Characteristic Ice Shapes

Cross-sectional ice shapes on turning vanes A and B are illustrated in figures 12(a) and (b). Three important observations result from this figure. First, both sets of turning vanes accreted ice at the leading edge and along the pressure surface. Furthermore for all cases, excluding the 45 μm DVM spray on vanes A, a thin layer of frost formed on the suction surface. A thin layer of glaze ice formed on the suction surface for the 45 μm case on turning vanes A. Glaze ice formed on turning vanes A for the 45 and 30 μm DVM cloud. All other conditions resulted in rime ice. Second, by contrasting the ice accretion on turning vanes A and B, one can see that the amount of ice accretion on vanes A varies dramatically with drop size, while remaining fairly constant on turning vanes B. Third, figures 12(a) and (b) show that vanes A can accrete very severe ice shapes (45 and 30 μm sprays); loss coefficient can increased by a factor of 5.4 (ref. 2). The dry loss coefficient, $C_{D,CLEAN}$, was about 0.33 at a test section velocity of 112 m/sec. Figure 13, from reference 2, shows the loss coefficient increase as a function of ice accretion time for an

extremely severe icing condition. On the other hand, the ice shapes on vanes B were never too severe. The ice shapes on B for the 40 min sprays were very much like the 10 min ice accretion on turning vanes A. Reference 2 showed that a 10 min spray on vanes A cause a factor of 1.5 increase in the loss coefficient.[3] The rime ice on the leading edge of vanes B varied from 6.4 to 12.7 mm thick for the four sprays.

Ice shapes on the fan blades at three different radial positions are shown on figure 14. The ice was a mixture of glaze and rime ice. These cross-sectional tracings show that the ice accretion was relatively independent of drop size. The ice thicknesses at the stagnation point for the four sprays varied from 9.5 to 25.4 mm. These ice shapes also demonstrate that significant amounts of ice can accrete on the fan blades.

These two sets of ice shapes show that (1) turning vanes require ice protection at the leading edge and along the pressure surface, and (2) the fan blades may require some form of ice protection. Analytic droplet trajectory calculations have shown that (1) will hold true for AWT diffusion control turning vanes. The AWT fan blades will experience more severe ice accretion due to the higher tip Mach numbers (0.3 in IRI to 0.7 in AWT). Thus, one would expect both more blade damage from shed ice and also more severe aeropenalties in the AWT due to increased blade ice accretion and higher blade velocities.

Overall Total Collection Efficiency Curve for Vanes A

The overall total collection efficiency, E, is defined as the total amount of mass removed by the entire array of turning vanes A, MV, divided by the total mass of cloud reaching the turning vanes, MC - equation (1).

$$E = \frac{MV}{MC} \tag{1}$$

The collection efficiency curve for turning vanes A is shown in figure 15. E was determined experimentally by measuring MV for the four DVM sprays and we knew MC based on the water flow rate into the tunnel and the time of the spray. The term Ko, plotted on the x-axis, is a dimensionless inertia parameter and is a function of drop size, d, air velocity, V, and body geometry, C, ($Ko \propto V^{0.6} d^{1.6}/C$). Ko was calculated based on the DVM of each spray and assuming a one-dimensional velocity profile. Chapter 2 in the "Engineering Summary of Airframe Icing Technical Data," ADS-4, discusses two methods to calculate Ko (ref. 3). Both methods proved straightforward; the method used in the calculations presented here was the graphical method. The perpendicular distance between two adjacent turning vanes was selected as the proper characteristic length. This length was 0.23 m for the IRT turning vanes A and 0.35 m for the AWT turning vanes (diffuser control vanes).

---

[3]The loss coefficient was defined as the total pressure loss obtained from integrating the area enclosed by the appropriate upstream and downstream transverse profiles divided by the local upstream dynamic pressure.

The four data points indicated on figure 15 represent the four DVM sprays run in the IRT test. The less than 10 μm spray has the lowest Ko and E values, while the 45 μm case has the largest values of Ko and E. The collection efficiency curve reflects the strong influence drop size has on the total overall catch efficiency. The curve has a very steep slope with the larger drop sizes (30 and 45 μm sprays) and flattens out for the smaller drop sizes (15 and <10 μm sprays).

One should note that E defined here differs slightly from the definition used in ADS-4 (ref. 3). ADS-4 defined E in terms of the rate of water droplet impingement/foot of span. In contrast, E here is defined in terms of the total amount of cloud removed by an entire array of turning vanes. Note also that it was not possible to calculate Ko for turning vanes B, IGVs, and fan blades since the DVM drop size changed and was unknown once the cloud passed corner A.

Mass Distribution

The results from the mass distribution gave the most surprising results. Contrary to what one would have expected from the pictorial walk around the IRT, the heat exchanger proved to be the primary remover of the cloud. For only one case did the heat exchanger remove less than 50 percent of the cloud. At a 45 μm DVM spray the heat exchanger and turning vanes A each removed about 47 percent of the cloud. For the less than 10 DVM μm spray the heat exchanger removed a whopping 90 percent of the total spray cloud. Figure 16 shows the contribution of each component in removing the spray cloud as a function of drop size. For the smaller drops some snow was found in both the fan and heat exchanger area. The contribution of the IGVs is not shown because they removed such a small percentage of the cloud the contribution could not accurately be shown. Notice that the figure shows that the percent of the cloud removed by both turning vanes B with FOD screen and the fan blade stayed relatively constant with drop side. This result is consistent with the invariance of ice shapes with DVM drop size sprays in figures 12(b) and 14. Note also that for all cases no ice was observed on turning vanes C.

The ice accretion on the FOD screen, albeit a small percentage of the total spray cloud, can cause a large enough pressure drop to require deicing. In the IRT the ice build up on the FOD screen occasionally must be manually deiced in order to achieve the desired test section velocity.

A likely scenario for why such a large percentage of the cloud reaches the heat exchanger with no ice accretion on turning vanes C is that the tunnel acts as a small pass filter, i.e., turning vanes A and B, IGVs, and fan blades catch the large droplets and allow the smaller ones to pass. This analogy explains why vanes A, which sees the largest percentage of big drops, accretes substantially more of the cloud than turning vanes B which sees a much smaller percentage of large drops.

To help clarify this scenario consider what happened to the spray cloud as it passed turning vanes A. The large droplets in the spray distribution had a much higher collection efficiency than the smaller drops due to the relation $Ko \propto d^{1.6}$. Thus turning vanes A removed a larger percentage of the big drops than the smaller drops by virtue of the higher collection efficiency. As a result the spray cloud downstream of the turning vanes contained essentially

the same number of the small drops and none of the largest drops. Consequently the capacity of turning vanes B, FOD screen, IGVs, and fan blades to remove the spray cloud was reduced substantially.

This scenario is applicable in the same exact manner to the remaining tunnel components. The reason the fan blades accrete more ice than the IGVs is due to the high blade velocities. No ice accreted on turning vanes C because the cloud, at this point, contains only very small droplets which together with the low velocities lack the necessary inertia to deviate from the airflow streamlines and therefore to accrete on the vanes. However, the heat exchanger's thin fins with their near unity collection efficiencies in conjunction with the large area covered by the fins provide sufficient geometry to remove the remaining portion of the spray cloud.

Although this explanation of the mass distribution results is a scenario, it nevertheless, provides the most probable explanation for why such a large percentage of the cloud reached the heat exchanger.

PROJECTION TO AWT

The mass distribution of ice among the IRT components was projected to the AWT to account for its larger physical size and higher velocities. In addition an estimate was made for a "worst case" icing condition on turning vanes 1 in the AWT.

Two assumptions were made in making the projections. They were (1) the velocity, drop size, and LWC spacial distributions in the IRT and AWT are similar, and (2) the overall total collection efficiency curve for turning vanes A in the IRT holds for the diffuser control turning vanes in the AWT.

Mass Distribution

The projection of the mass distribution was based on a test section Mach number of 0.6 (0.3 in corner 1). This Mach number was selected because it represents the upper speed limit in the commercial and business jet flight envelope for hold conditions. A brief discussion on how the projection was made for the various tunnel components is given below.

Scaling the percent of the cloud removed by the first set of turning vanes simply involved, calculating Ko for the AWT turning vanes at a Mach number of 0.3 for various drop sizes, and reading E off figure 15. E multiplied by 100 is precisely that percent. A linear extrapolation of the catch curve was assumed for the cases where Ko exceeded the Kos of the IRT data. The second set of turning vanes was scaled by increasing the percent cloud removed by the same percent increase for the first set of turning vanes. The mass of ice accretion on the fan blades was scaled based on the dimensionless inertia parameter equation, ($Ko \propto V^{0.6}d^{1.6}/C$) - equation (2) was the equation used.

$$MFawt = 2MFirt \frac{NBawt}{NBirt} \frac{Cirt}{Cawt} \left(\frac{MTawt}{MTirt}\right)^{0.6} \qquad (2)$$

Here MF is the weight of ice on the fan blades, NB is the number of blades/stage, C is the cord length, and MT is the tip Mach number. The multiple 2 is needed since the AWT fan will have two stages. The percent of the cloud removed by the heat exchanger is the remaining portion of the cloud. The resulting mass balance scaled to the AWT is shown in figure 17. Notice that the heat exchanger still removes a very large percentage of the spray cloud, especially for small droplet sprays.

Three comments need to be made concerning the mass balance scaling. First, the uncertainties inherent in the assumptions made for scaling the second set of turning vanes and the fan blades are minimized due to the small percent of the cloud they removed in the IRT, i.e., the assumptions would have to cause a very large error in order to affect the predicted mass balance in the AWT. Second, the relatively small percent of the cloud removed by the fan blades does not imply ice protection is not necessary. Rather, figure 13 in conjunction with the increased fan blade velocities and ice shedding in the AWT suggest the necessity of ice protection for the fan blades. Third, the estimated percent of the spray cloud removed by the AWT heat exchanger is not affected by the fact that it will be located upstream of the third set of turning vanes. This is true since for all four DVM sprays no ice accreted on turning vanes C in the IRT. Thus, the IRT and AWT heat exchanger locations are directly analogous.

A "Worst Case" Icing Condition

A "worst case" icing condition for turning vanes 1 can have no precise definition. The validity of this assertion rests in the fact that one can always spray for a longer period than a previously defined "worst case." In the limit, the ice accreted on turning vanes 1 could completely block the tunnel air flow.

In lieu of a precise definition of a "worst case" icing condition a practical definition was established based on typical hold conditions in the commercial and business jet flight envelopes. A typical hold condition which would likely be tested in an icing facility are: LWC = 0.5 g/m^3, MVD = 25 μm, Mach number = 0.5, and spray time = 45 min. Under these conditions approximately 2090 kg (4600 lb) of ice will accrete on turning vanes 1 in the AWT. This condition represents the longest spray which will be used in the AWT for a single data point.

The significance of 2090 kg of ice on turning vanes 1 in the AWT resides in the resulting increase in the total pressure loss due to the ice build up. An estimation of the pressure loss increase was made by (1) assuming the drag increase is primarily caused by blockage between adjacent turning vanes, (2) accounting for the difference in ice accretion surface area between AWT turning vanes and IRT turning vanes, and (3) using figure 13 to find the increase in loss coefficient. Step (2) was necessary to go from 2090 kg of ice accretion on turning vanes 1 in AWT to an equivalent ice accretion in the IRT from which total pressure loss data were available.

Following the above procedure an equivalent icing time in the IRT was 61 min for the tunnel conditions in figure 13. Extrapolating the curve in figure 13 out to 61 min indicates a factor of 7 increase in the turning vane A loss coefficient. This factor of 7 increase is the estimate for the increase

in loss coefficient for turning vanes 1 in the AWT. The clean loss coefficient for the AWT turning vanes was measured to be 0.12 (ref. 4). Note that this estimation assumes similar flow conditions in the first turn, geometrically similar turning vanes, and no compressibility effects. These three assumptions were necessary in order to gain some understanding of the significance of the "worst case" icing condition.

SUMMARY OF RESULTS

1. The most important and surprising result from the IRT test was the overall mass distribution of ice among the tunnel components and its projection to the AWT. The implication for the AWT design is that the heat exchanger must have the capacity of handling from 50 to 90 percent of the total spray cloud without plugging up or reducing the overall heat transfer rate to the point where tunnel shutdown is required.

2. The ice shapes on the two sets of turning vanes A and B showed that ice protection will only be necessary along the pressure surface and at the stagnation point. Analytic droplet trajectory calculations have shown that this conclusion holds for the proposed diffusion control vanes for the AWT. Ice protection on the second set of turning vanes may not be needed depending on what is an acceptable total pressure loss. It is the opinion of the authors that at most the leading edge region requires ice protection.

3. The ice shapes on the fan blades showed that significant amount of ice will accrete on the fan blades. In order to ensure both efficient tunnel operation and the maintenance of fan blades, an ice protection system is necessary for the AWT due to the higher blade Mach numbers and the double stage fan.

4. The FOD screen did not remove a substantial portion of the spray cloud. However, past experience in the IRT has shown that ice formation on the screen can cause enough of a pressure drop to require manual deicing. This same result will likely occur in the AWT.

REFERENCES

1. Olsen, W.; Shaw, R.; and Newton J.: Ice Shapes and the Resultant Drag Increase for a NACA 0012 Airfoil. NASA TM-83556, 1984.

2. Cubbison, R.W.; and Newton, J.E.; and Schabes, H.L.: Losses Across the Icing Research Tunnel "A" Corner and the Increase in Loss Due to Ice Accretion on the Turning Vanes. NASA Lewis Research Center, In-House Report, 1984.

3. Bowden, D.T.; Gensemer, A.E.; and Skeen, C.A.: Engineering Summary of Airframe Icing Technical Data. Federal Aviation Agency, FAA-ADS-4, Mar. 1964.

4. Gelder, T.; Moore, J.; and Sanz J.: Wind Tunnel Turning Vanes of Modern Design. NASA TM-87416, 1986.

TABLE I

DVM, μm	LWC, g/m^3	τ, min	V, m/sec	To, c
10	0.5	78.5	67	-12
15	1.36	39.25	67	-12
30	1.36	39.25	67	-12
45	1.92	27.8	67	-12

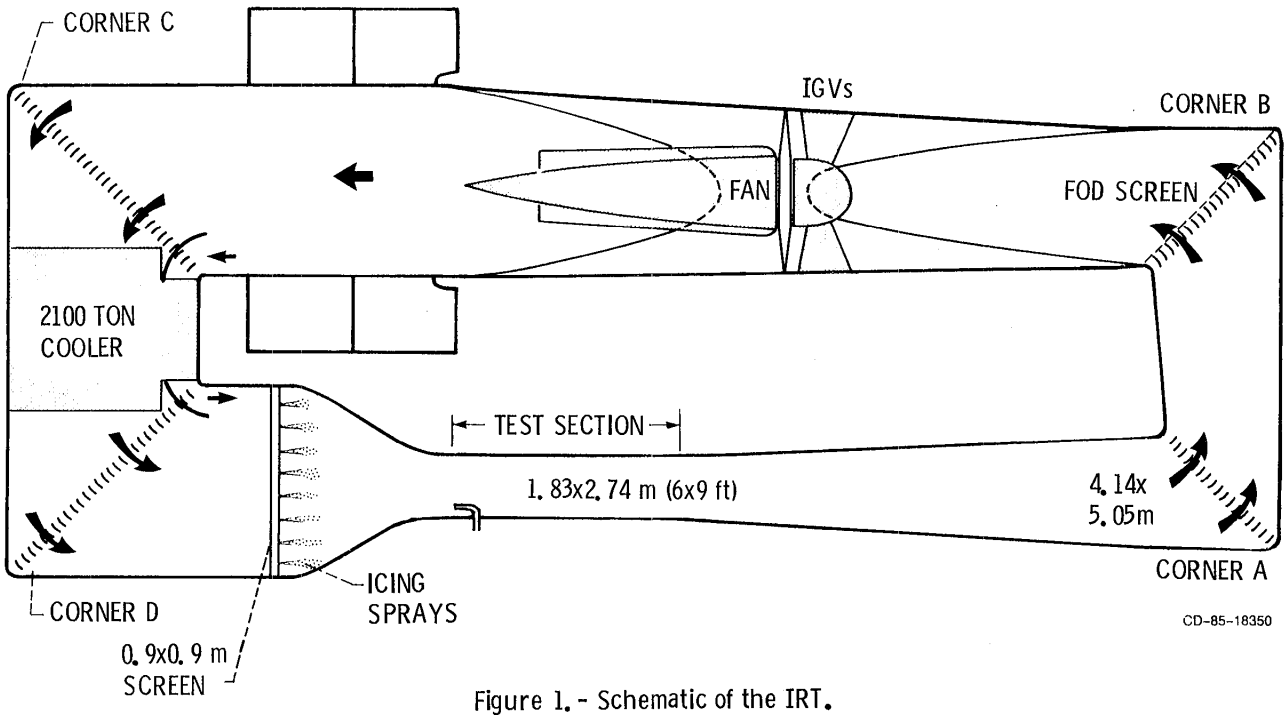

Figure 1. - Schematic of the IRT.

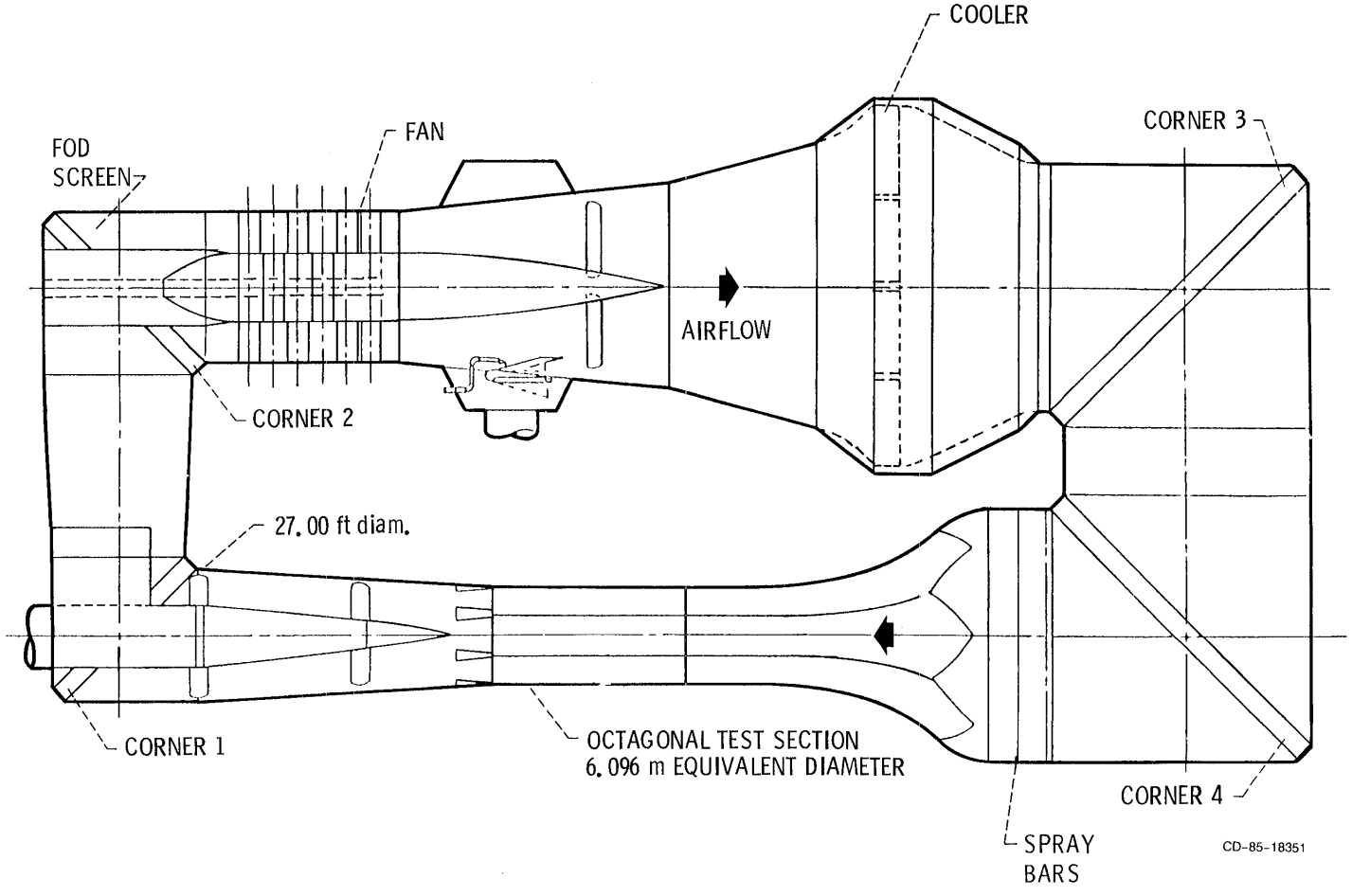

Figure 2. - Schematic of the AWT.

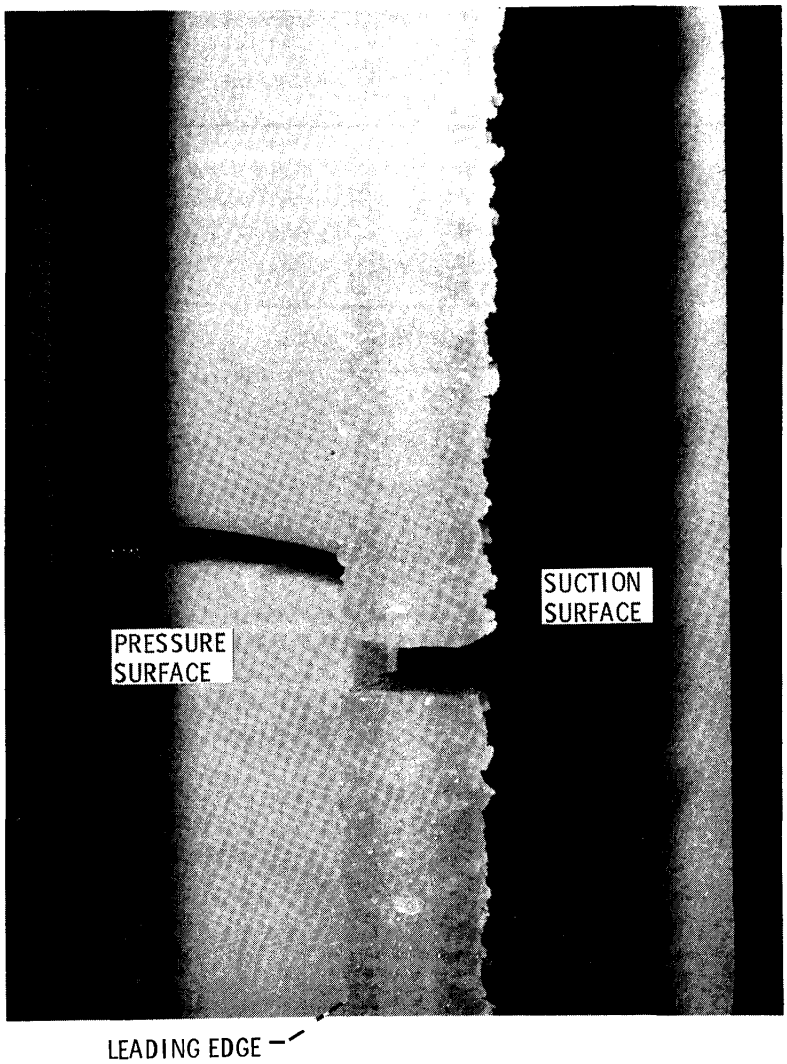

Figure 3. - Ice accretion on turning vanes A; V = 67.1 m/s, $T_0 = -12\ ^{o}C$, LWC = 1.36 g/m^3, τ = 39.25 min., DVM = 30 μm.

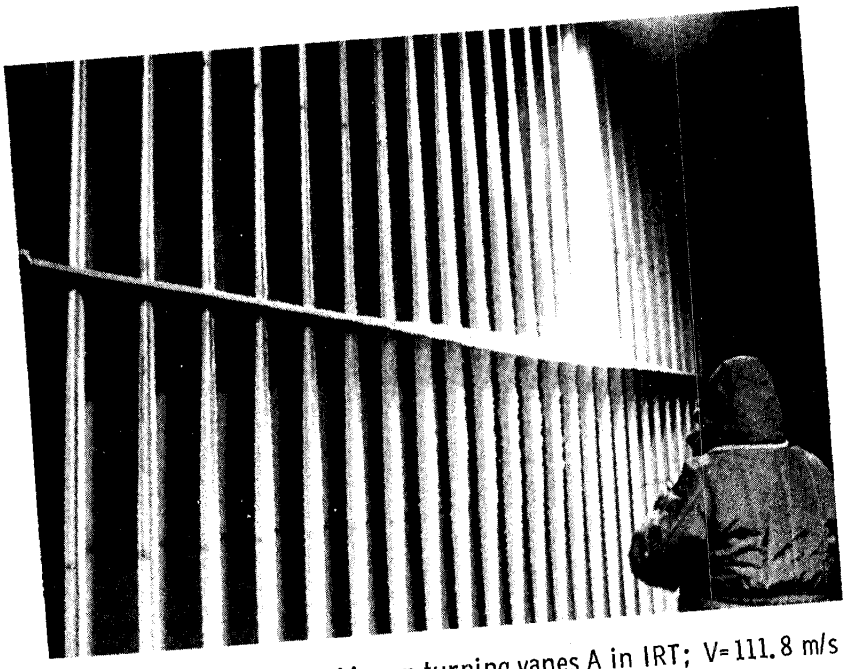

Figure 4. - Distribution of ice on turning vanes A in IRT; V=111.8 m/s To=-7 ^{o}C, LWC=1.1 g/m^{3}.

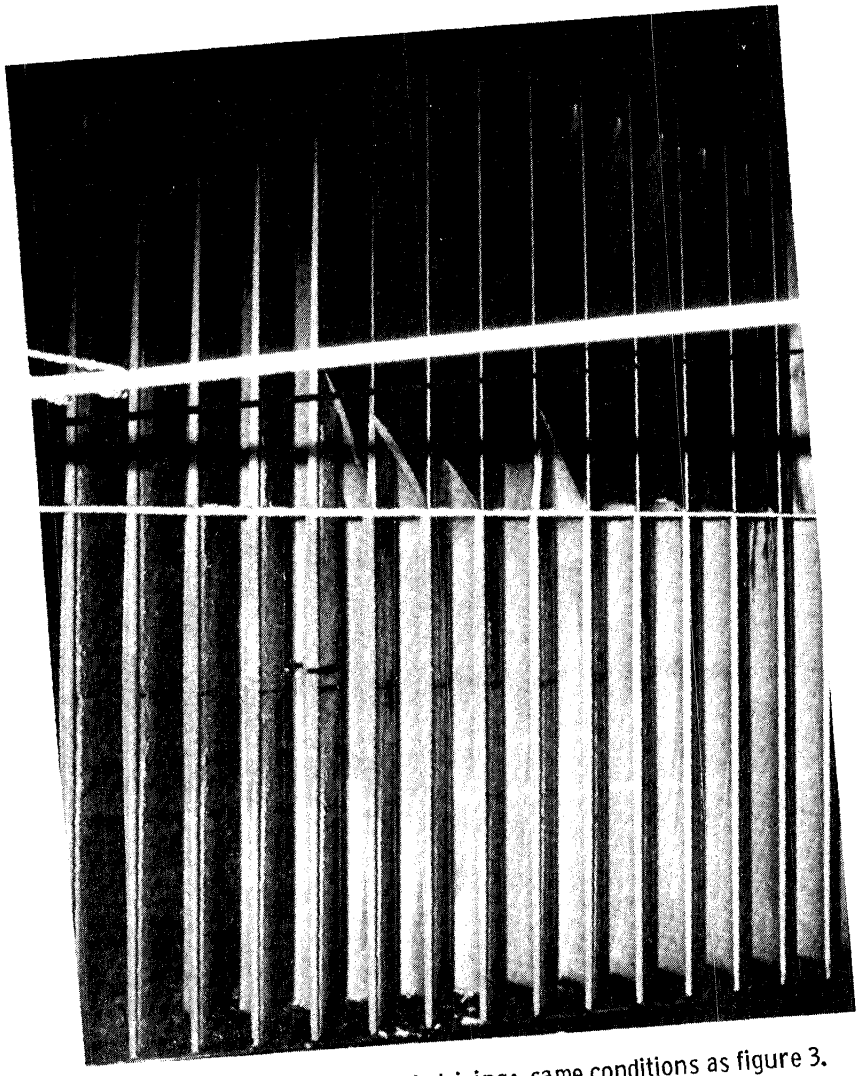

Figure 5. - Turning vanes A deicing; same conditions as figure 3.

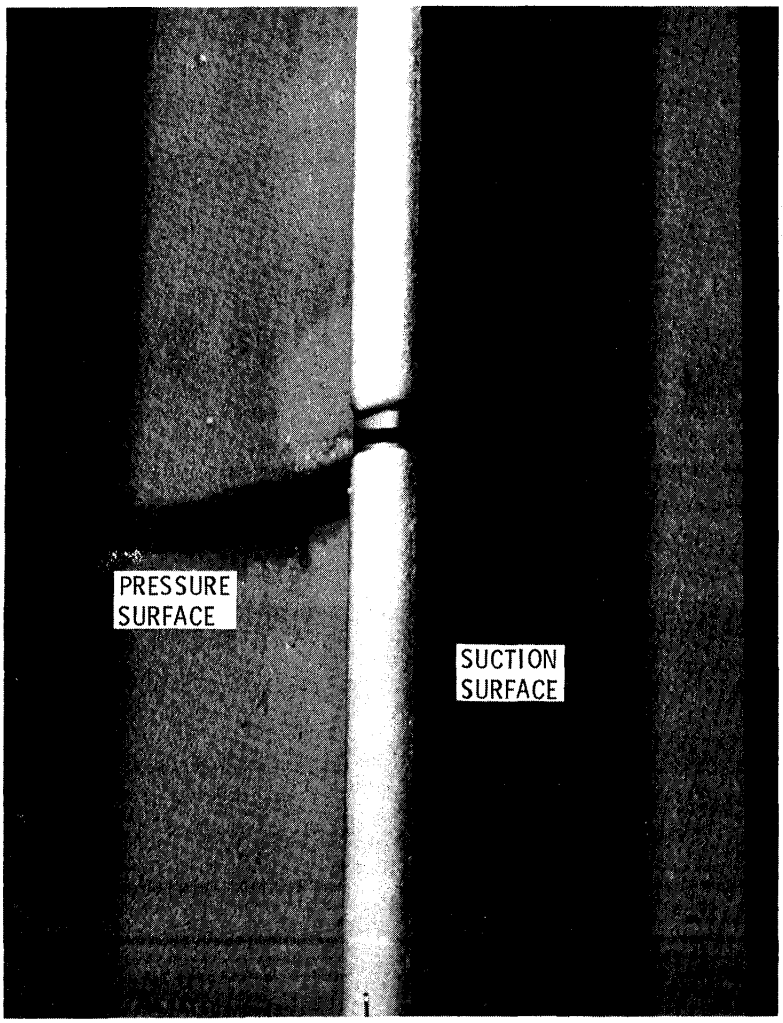

Figure 6. - Ice accretion on turning vanes B; same conditions as figure 3.

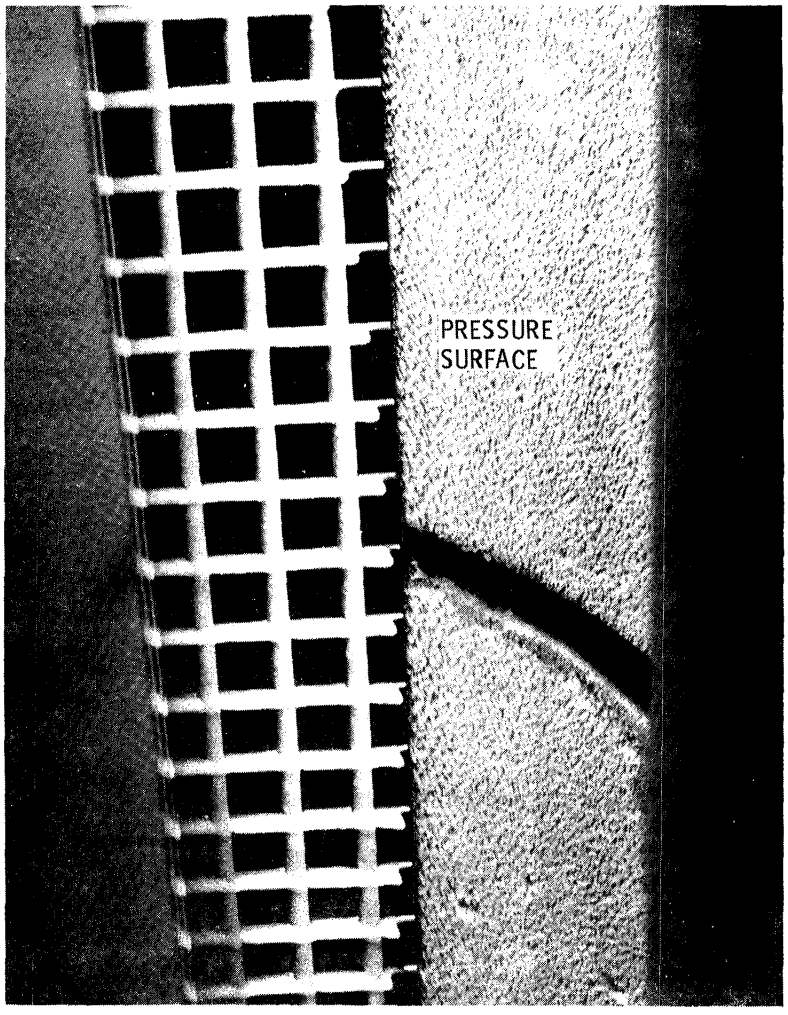

Figure 7. - Ice accretion on FOD screen and pressure surface of turning vane B; same conditions as figure 3.

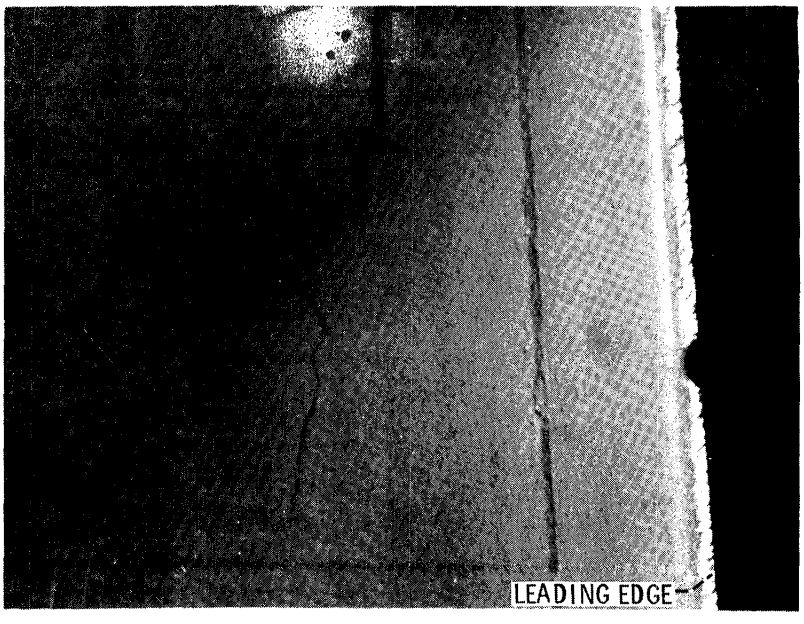

Figure 8. - Ice accretion on IGVs; DVM=15 microns, all other conditions are the same as conditions in figure 3.

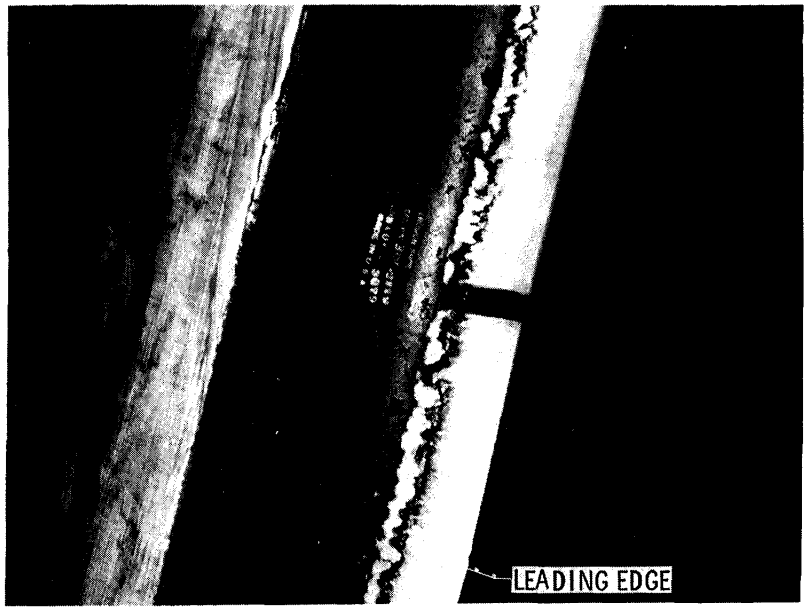

Figure 9. - Ice accretion on fan blade; conditions same as figure 8.

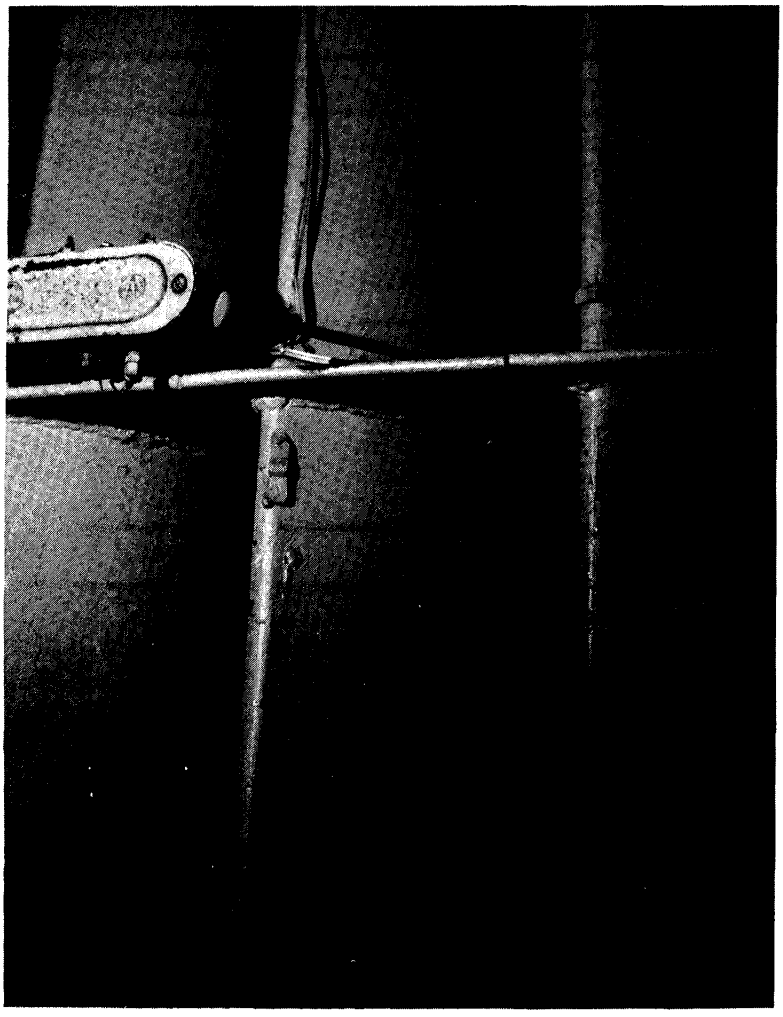

Figure 10. - Turning vane C; conditions same as figure 8.

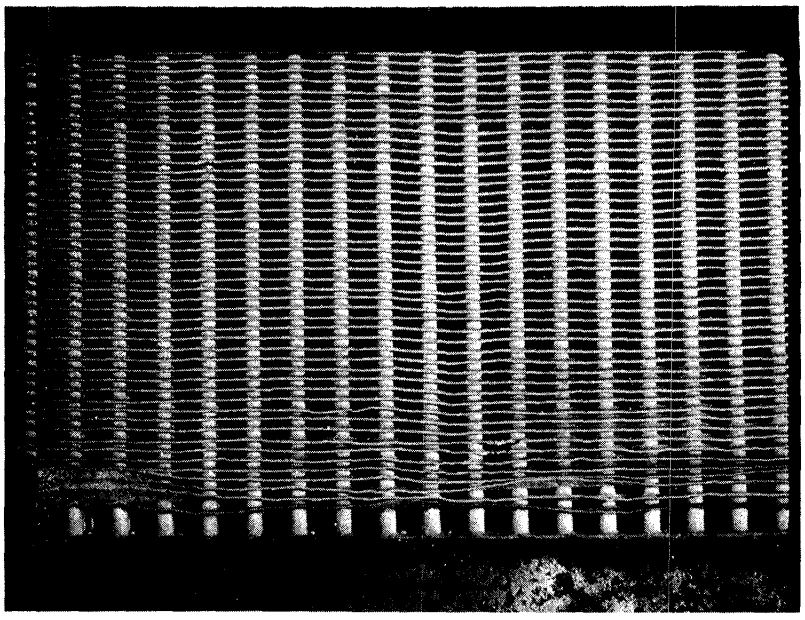

Figure 11. - Ice accretion on the heat exchanger; conditions same as figure 8.

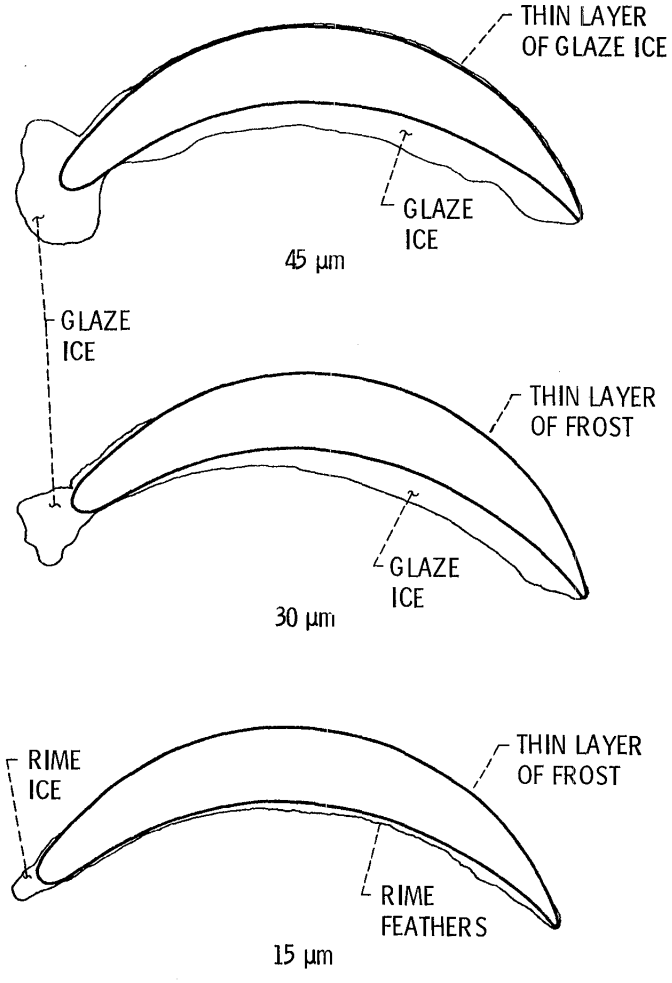

(a) Ice shapes on IRT turning vanes A; V = 67.1 m/s; T_0 = - 12 ^{o}C; LWCxVxτ = 214.8 kg/m^2.

Figure 12.

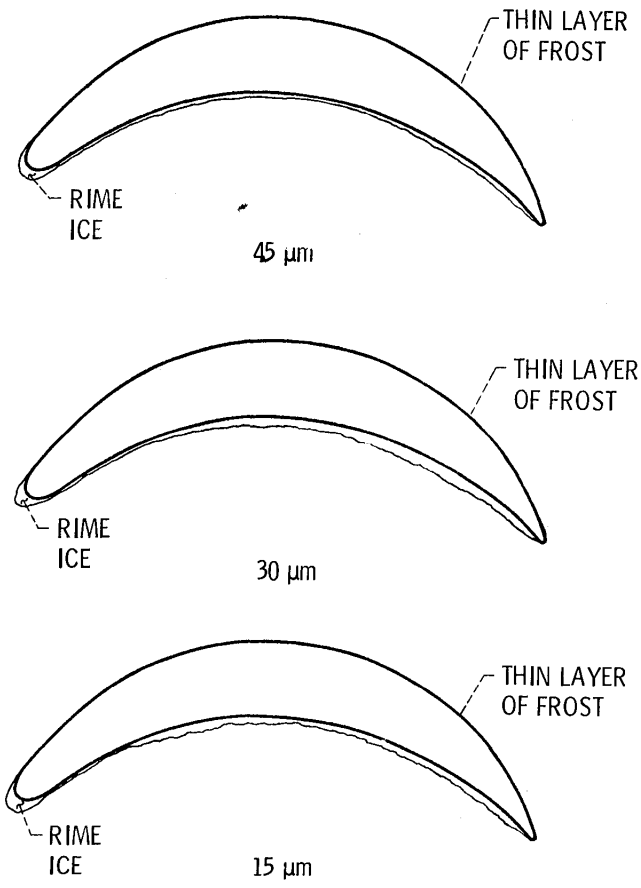

(b) Ice shapes on IRT turning vanes B; $V = 67.1$ m/s; $T_0 = -12\ ^{o}C$; $LWC \times V \times \tau = 214.8\ kg/m^2$.

Figure 12. - Concluded.

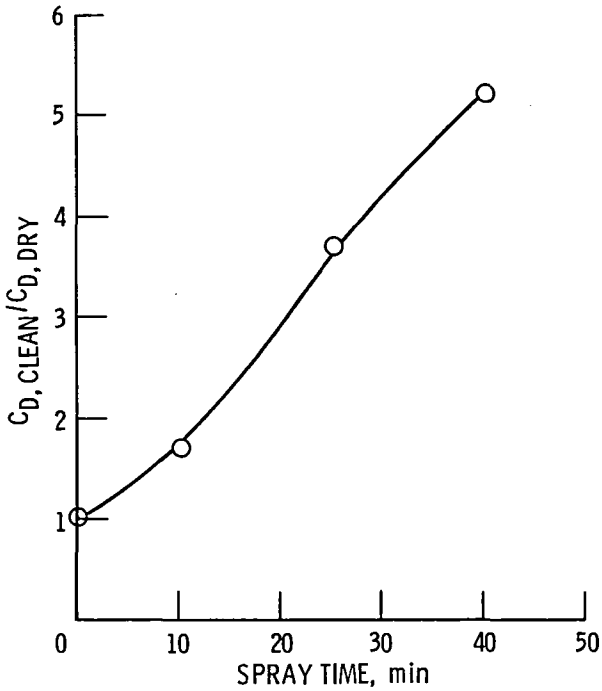

Figure 13. - Effect of glaze ice growth on loss coefficient across IRT A turning vanes; LWC = 1.1 g/m^3, DVM = 31 μm; T_0 = -7 °C, V = 112 m/s.

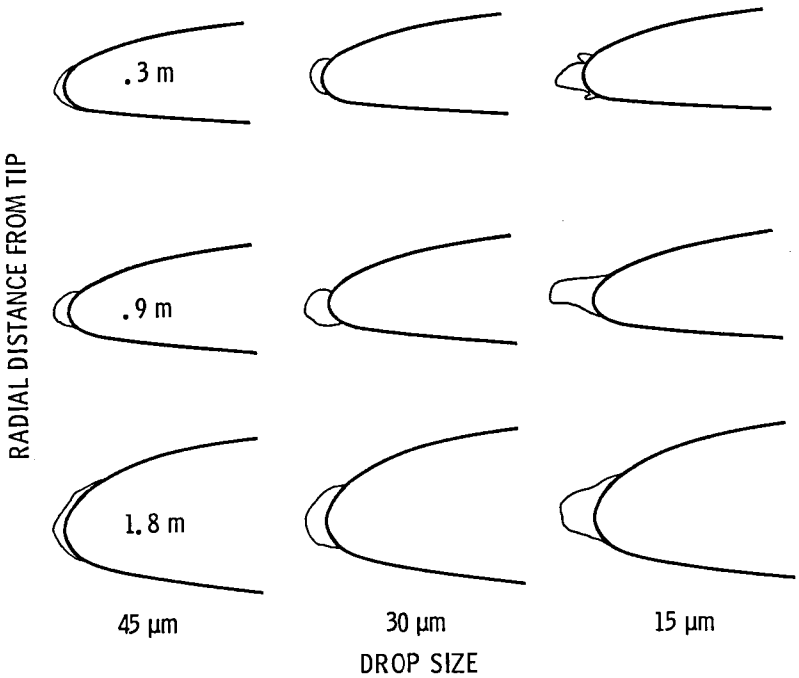

Figure 14. - Ice shapes on IRT fan blades; V = 67.1 m/s, T_0 = - 12 °C, LWCxVxτ = 214.8 kg/m^2.

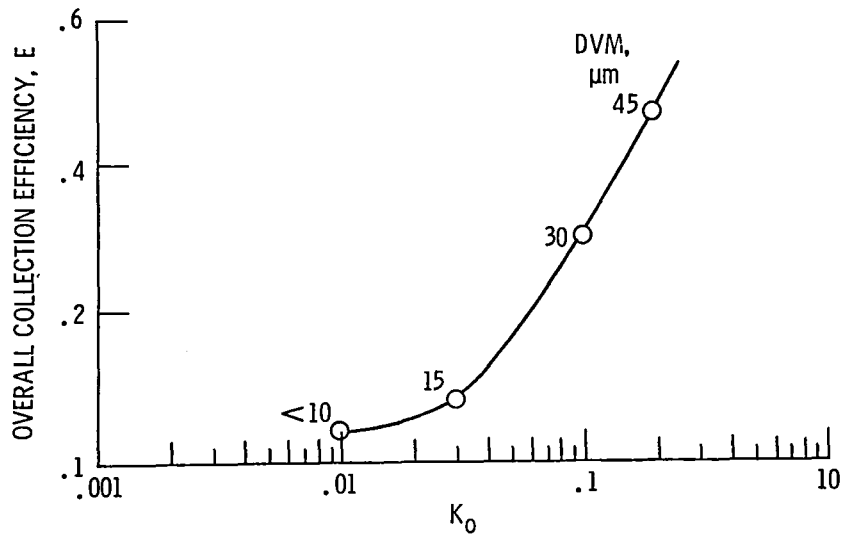

Figure 15.- Overall total collection efficiency curve for IRT turning vanes.

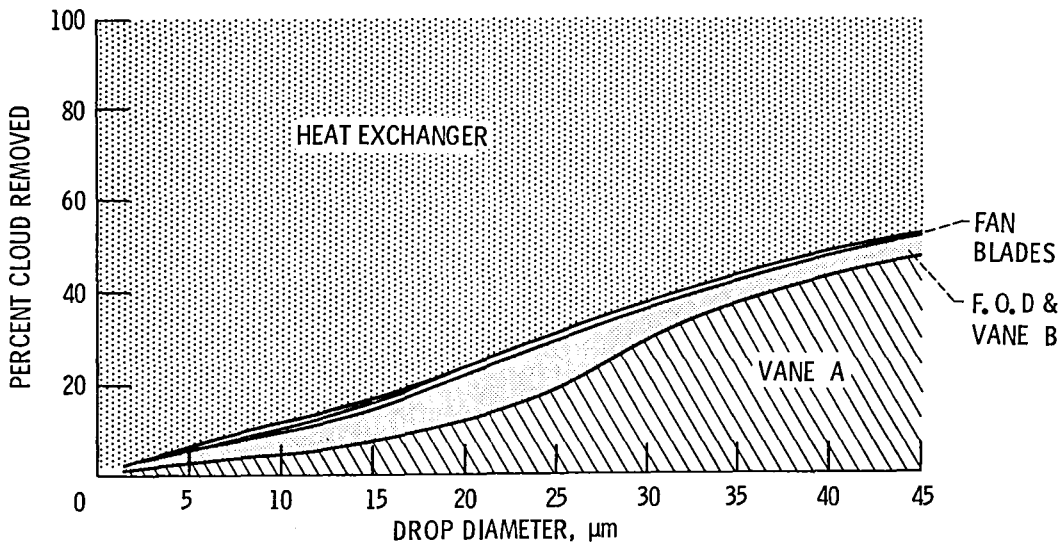

Figure 16. - Mass distribution in the IRT; V = 67.1 m/s; T_0 = - 12 °C.

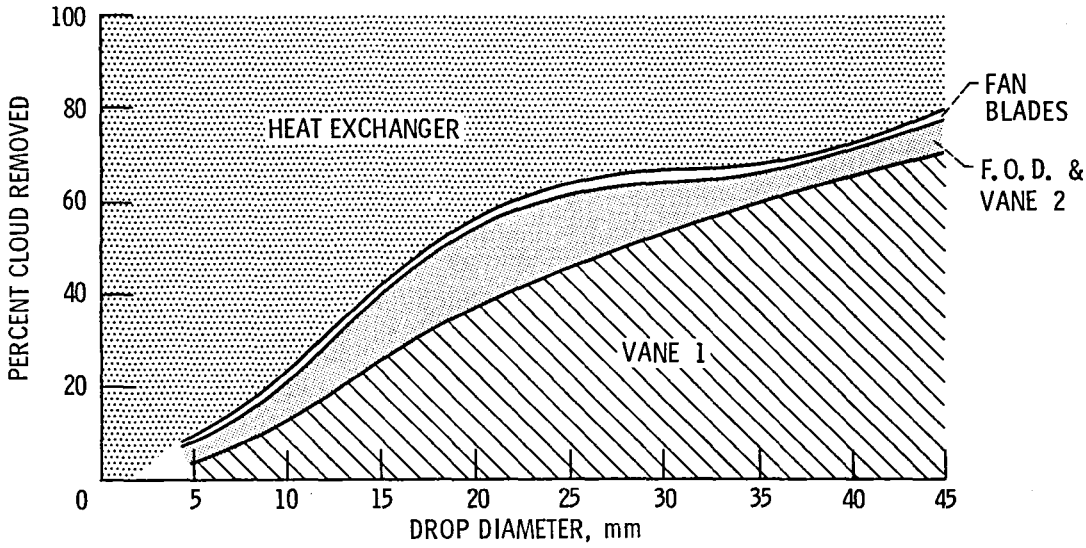

Figure 17. - Mass distribution scaled from IRT results to the AWT; test section Mach number = 0.6.

1. Report No.	2. Government Accession No.	3. Recipient's Catalog No.
NASA TM-87095		

4. Title and Subtitle	5. Report Date
Study of Ice Accretion on Icing Wind Tunnel Components	6. Performing Organization Code: 505-45-54

7. Author(s)	8. Performing Organization Report No.
James E. Newton and William Olsen	E-2838
	10. Work Unit No.

9. Performing Organization Name and Address	11. Contract or Grant No.
National Aeronautics and Space Administration Lewis Research Center Cleveland, Ohio 44135	13. Type of Report and Period Covered: Technical Memorandum

12. Sponsoring Agency Name and Address	14. Sponsoring Agency Code
National Aeronautics and Space Administration Washington, D.C. 20546	

15. Supplementary Notes

Prepared for the Twenty-fourth Aerospace Sciences Meeting, sponsored by the American Institute of Aeronautics and Astronautics, Reno, Nevada, January 6-8, 1986.

16. Abstract

In a closed loop icing wind tunnel the icing cloud is simulated by introducing tiny water droplets through an array of nozzles upstream of the test section. This cloud will form ice on all tunnel components (e.g., turning vanes, inlet guide vanes, fan blades, and the heat exchanger) as the cloud flows around the tunnel. These components must have the capacity to handle their icing loads without causing significant tunnel performance degradation during the course of an evening's run. To aid in the design of these components for the proposed Altitude Wind Tunnel (AWT) at NASA Lewis Research Center the existing Icing Research Tunnel (IRT) was used to measure icing characteristics of the IRT s components. The results from the IRT were scaled to the AWT to account for the AWT's larger components and higher velocities. The results showed that from 90 to 45 percent of the total spray cloud froze out on the heat exchanger. Furthermore, the first set of turning vanes downstream of the test section, the FOD screen and the fan blades showed significant ice formation. The scaling showed that the same results would occur in the AWT.

17. Key Words (Suggested by Author(s))	18. Distribution Statement
Icing; Wind tunnel; Tunnel component icing	Unclassified - unlimited STAR Category 09

19. Security Classif. (of this report)	20. Security Classif. (of this page)	21. No. of pages	22. Price*
Unclassified	Unclassified		

*For sale by the National Technical Information Service, Springfield, Virginia 22161

End of Document